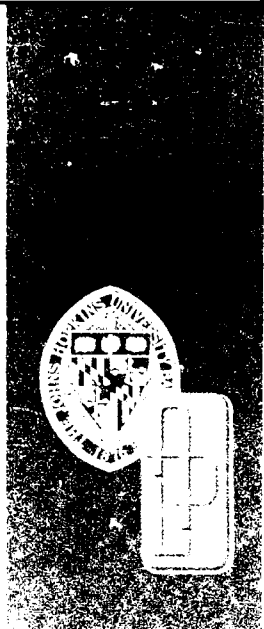


JHU/APL
TG 1375
SEPTEMBER 1989
Copy No.



(4)

AD-A213 925

Technical Memorandum

RECTANGULAR-TO-CIRCULAR WAVEGUIDE TRANSITIONS FOR HIGH-POWER CIRCULAR OVERMODED WAVEGUIDES

WILLIAM A. HUTING

DTIC
ELECTED
OCT 31 1989
S B D
CD

JOHNS HOPKINS UNIVERSITY ■ APPLIED PHYSICS LABORATORY

Approved for public release; distribution is unlimited

210

JHU/APL
TG 1375
SEPTEMBER 1989
Copy No.

RECTANGULAR-TO-CIRCULAR WAVEGUIDE TRANSITIONS FOR HIGH-POWER CIRCULAR OVERMODED WAVEGUIDES

WILLIAM A. HUTING

Approved for public release; distribution is unlimited.

UNCLASSIFIED

SECURITY CLASSIFICATION OF THIS PAGE

REPORT DOCUMENTATION PAGE

1a. REPORT SECURITY CLASSIFICATION Unclassified		1b. RESTRICTIVE MARKINGS																									
2a. SECURITY CLASSIFICATION AUTHORITY		3. DISTRIBUTION/AVAILABILITY OF REPORT Approved for public release; distribution unlimited																									
2b. DECLASSIFICATION/DOWNGRADING SCHEDULE																											
4. PERFORMING ORGANIZATION NUMBER(S) JHU/APL TG 1375		5. MONITORING ORGANIZATION REPORT NUMBER(S) JHU/APL TG 1375																									
6a. NAME OF PERFORMING ORGANIZATION The Johns Hopkins University Applied Physics Laboratory		6b. OFFICE SYMBOL (If Applicable) F2B	7a. NAME OF MONITORING ORGANIZATION NAVPRO, Laurel, Maryland																								
6c. ADDRESS (City, State, and ZIP Code)		7b. ADDRESS (City, State, and ZIP Code) Johns Hopkins Road Laurel, Maryland 20707																									
8a. NAME OF FUNDING/SPONSORING ORGANIZATION NAVSEA		8b. OFFICE SYMBOL (If Applicable) PMS-400B	9. PROCUREMENT INSTRUMENT IDENTIFICATION NUMBER N00039-89-C-5301																								
8c. ADDRESS (City, State, and ZIP Code) Johns Hopkins Road Laurel, Maryland 20707		10. SOURCE OF FUNDING NUMBERS																									
		PROGRAM ELEMENT NO.	PROJECT NO.																								
		TASK NO.	WORK UNIT ACCESSION NO.																								
11. TITLE (Include Security Classification) Rectangular-to-Circular Waveguide Transitions for High-Power Overmoded Waveguides																											
12. PERSONAL AUTHOR(S) Huting, William A.																											
13a. TYPE OF REPORT Technical Memorandum	13b. TIME COVERED FROM 0/00 TO 0:00	14. DATE OF REPORT (Year, Month, Day) September 1989	15. PAGE COUNT 30																								
16. SUPPLEMENTARY NOTATION																											
17. COSATI CODES	18. SUBJECT TERMS <table border="0"> <tr> <td>FIELD</td> <td>GROJP</td> <td>SUB-GROUP</td> <td>Communication</td> <td>Power</td> <td>Waveguides</td> </tr> <tr> <td></td> <td></td> <td></td> <td>Microwaves</td> <td>Radar</td> <td></td> </tr> <tr> <td></td> <td></td> <td></td> <td>Modes</td> <td>Transitions</td> <td></td> </tr> <tr> <td></td> <td></td> <td></td> <td>Overmoded</td> <td>Transmission</td> <td></td> </tr> </table>			FIELD	GROJP	SUB-GROUP	Communication	Power	Waveguides				Microwaves	Radar					Modes	Transitions					Overmoded	Transmission	
FIELD	GROJP	SUB-GROUP	Communication	Power	Waveguides																						
			Microwaves	Radar																							
			Modes	Transitions																							
			Overmoded	Transmission																							
19. ABSTRACT (Continue on reverse if necessary and identify by block number) <p>Circular overmoded waveguide is being investigated at The Johns Hopkins University Applied Physics Laboratory (JHU/APL) for low loss, high power microwave transmission near 3.0 GHz. Unfortunately, most microwave power sources and receivers are compatible with single-mode rectangular waveguide rather than overmoded circular waveguide. This problem is usually solved by using metallic waveguide transitions. Design objectives for such transitions include high power-carrying capability, low mode conversion, low reflectivity, and low transmission loss. An overview of the theory of waveguide transition operation is presented. It is concluded that a prerequisite for a comprehensive waveguide transition analysis is to solve the uniform waveguide problem for the various cross sections of the transition. A review is included that describes some of the difficulties encountered in developing a computer program package that analyzes uniform waveguides with arbitrary cross sections. An overview is included of important waveguide design issues, several proposed designs, and several different tasks and problem areas one might encounter in a long-term study.</p>																											
20. DISTRIBUTION/AVAILABILITY OF ABSTRACT <input checked="" type="checkbox"/> UNCLASSIFIED/UNLIMITED <input type="checkbox"/> SAME AS RPT <input type="checkbox"/> DTIC USERS		21. ABSTRACT SECURITY CLASSIFICATION Unclassified																									
22a. NAME OF RESPONSIBLE INDIVIDUAL NAVPRO Security Officer		22b. TELEPHONE (Include Area Code) (301) 953-5442	22c. OFFICE SYMBOL SE																								

ABSTRACT

Circular overmoded waveguide is being investigated at The Johns Hopkins University Applied Physics Laboratory (JHU/APL) for low loss, high power microwave transmission near 3.0 GHz. Unfortunately, most microwave power sources and receivers are compatible with single-mode rectangular waveguide rather than overmoded circular waveguide. This problem is usually solved by using metallic waveguide transitions. Design objectives for such transitions include high power-carrying capability, low mode conversion, low reflectivity, and low transmission loss. An overview of the theory of waveguide transition operation is presented. It is concluded that a prerequisite for a comprehensive waveguide transition analysis is to solve the uniform waveguide problem for the various cross sections of the transition. A review is included that describes some of the difficulties encountered in developing a computer program package that analyzes uniform waveguides with arbitrary cross sections. An overview is included of important waveguide design issues, several proposed designs, and several different tasks and problem areas one might encounter in a long-term study.



Accession For	
NTIS GRA&I	<input checked="" type="checkbox"/>
DTIC TAB	<input type="checkbox"/>
Unannounced	<input type="checkbox"/>
Justification	
By	
Distribution/	
Availability Codes	
Dist	Avail and/or Special
A-1	

CONTENTS

List of Illustrations	v
1. INTRODUCTION	1
2. WAVEGUIDE TRANSITION THEORY	7
3. COMPUTER SOFTWARE DEVELOPMENT	17
4. FUTURE WORK	21
References	23

ILLUSTRATIONS

1 Sheathed-helix waveguide	1
2 Multiport rectangular TE_{10} to circular TE_{01} mode transducer	2
3 Desired electric field lines for the multiport rectangular TE_{10} to circular TE_{01} mode transducer	3
4 Mode-transducing elbow	4
5 The Marie transducer	5
6 Desired electric fields for the Marie transducer	5
7 Generalized waveguide transition geometry	7
8 Waveguide transition geometry for electromagnetic field boundary conditions	13
9 Waveguide cross section approximated as a union of triangles	18
10 Nonuniform waveguide with transverse planes	19
11 Computer program package for scattering matrix determination	20
12 Waveguide run with regions capable of supporting a spurious mode	22
13 Waveguide run in which some of the spurious mode resonances have been eliminated	22

1. INTRODUCTION

The sheathed-helix waveguide (Fig. 1) that is being investigated at APL for low loss, high power microwave transmission¹ consists of a closely wound insulated wire surrounded by a two-layer jacket. The inner layer of the jacket is a lossy dielectric while the outer layer is a good conductor. Several short sections of this waveguide have been built at APL for use at S band (Table 1). Some of these sections are curved for use in 90° bends, while others are straight for use in straight waveguide runs. The purpose of the helix and the dielectric is to suppress all of the modes above cutoff except for the TE_{01} mode.

Microwave transmission using the TE_{01} mode of a circular waveguide is characterized by an attenuation that decreases monotonically with frequency. In order to achieve low attenuation and to minimize phase distortion, it is necessary to operate well above the TE_{01} cutoff frequency.² This implies that there are several modes above cutoff in addition to the four modes with cutoff frequencies less than or equal to that of the TE_{01} mode. One major design goal for the sheathed-helix waveguide

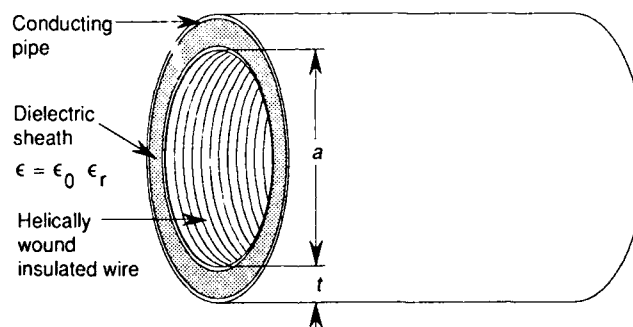


Figure 1 Sheathed-helix waveguide.

Table 1
Characteristics of overmoded waveguides built at APL.

Parameter (see Fig. 1)	Value
a	8.0 cm
t	0.8 cm
ϵ_r	5.2 – $j0.052$
f_{op}	3.0-3.6 GHz
Wire gauge	No. 14

¹W. A. Huting, J. A. Krill, and K. J. Webb, "New Developments in Circular Overmoded Waveguide," in 1988 URSI Radio Science Meeting Programs and Abstracts, International Union of Radio Science, Syracuse, N.Y., p. 202 (1988).

²H. E. Rowe and W. D. Warters, "Transmission in Multimode Waveguide with Random Imperfections," *Bell Syst. Tech. J.* **41**, 1031-1170 (1962).

is to avoid the transfer of energy from the TE_{01} mode to the other modes. These other modes are usually called "unwanted modes" or "spurious modes." The energy transferred to the spurious modes cannot be recovered because of dispersion and matching problems at the receiver. Therefore, significant spurious mode excitation could greatly increase transmission loss.

There are at least three major sources of coupling to spurious modes that must be considered in designing a run of overmoded waveguide. One of these sources is the presence of geometrical imperfections in the waveguide; an effort is now under way to investigate the effects of fabrication tolerances.^{1,2} The second major source of spurious mode excitation ("mode conversion") is the use of sharp bends in the waveguide run.³ Reference 3 gives a procedure for designing such bends for low mode conversion. The third source of mode conversion occurs (1) within the interface between the microwave power source and the waveguide run, and (2) within the interface between the waveguide run and the receiver. This additional mode conversion occurs because most microwave power sources and receivers are not compatible with circular overmoded waveguide. Rather, they are compatible with the dominant TE_{10} mode in standard-size rectangular waveguide.⁴ In order to match circular overmoded waveguide with such devices, it is necessary to use rectangular-to-circular waveguide mode transducers. Usually, such a mode transducer consists of a nonuniform waveguide whose cross section changes gradually along the longitudinal, or axial, dimension of the waveguide. In all nonuniform waveguides, some mode conversion is inevitable.^{5,6} Quantification of this mode conversion is an essential step in the evaluation of waveguide system performance. Furthermore, modification of existing waveguide transition designs may be necessary to achieve acceptable loss and power levels.

One waveguide transition that may be suitable for high power use has been proposed by Zinger and Krill.⁷ That transition (Fig. 2) is to be made out of copper or some other good conductor. The reason for the presence of four rectangular waveguide ports instead of only one (as in most previous designs) is that the power-carrying capability of circular waveguide may be more fully utilized for the waveguide sizes under consideration. Figure 3 illustrates the operation of this waveguide transition, showing the successive cross sections of the device, together with the electric field lines of the desired waveguide mode.

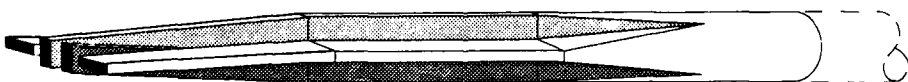


Figure 2 Multiport rectangular TE_{10} to circular TE_{01} mode transducer.

¹H.-G. Unger, "Normal Mode Bends for Circular Electric Waves," *Bell Syst. Tech. J.* **36**, 1292-1307 (1957).

²S. S. Saad, "Computer Analysis and Design of Gradually Tapered Waveguide with Arbitrary Cross Sections," Ph.D. dissertation, University College, London (Oct 1973).

³G. Reiter, "Generalized Telegraphist's Equation for Waveguides of Varying Cross Sections," *Proc. IEE* **106B**, Suppl. 13, 54-57 (1959).

⁴L. Solymer, "Spurious Mode Generation in Nonuniform Waveguide," *IRE Trans. Microwave Theory and Techniques* **MTT-7**, 379-383 (1959).

⁵W. H. Zinger and J. A. Krill, "Multiport Rectangular TE_{10} to Circular TE_{01} Mode Transducer Having Pyramidal Shaped Transducing Means," U.S. Patent No. 4,628,287 (9 Dec 1986).

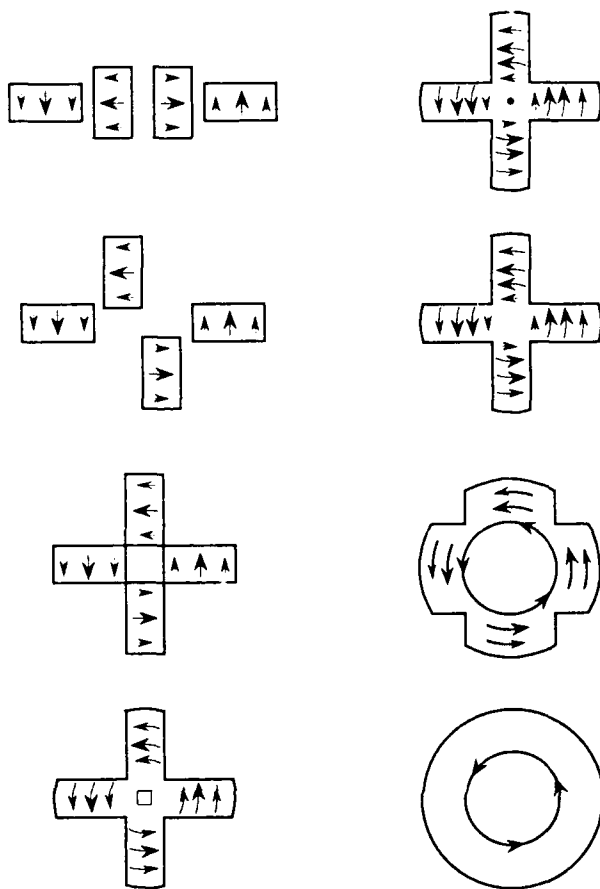


Figure 3 Desired electric field lines for the multiport rectangular TE_{10} to circular TE_{01} mode transducer.

As previously mentioned, another prominent source of mode conversion is the presence of sharp intentional bends in the waveguide. Tests at S band indicate that the helical waveguide bends made at APL are characterized by acceptable insertion losses and reflectivity levels.¹ Unfortunately, in order to avoid unsatisfactory levels of mode conversion, helical waveguide bends must be sufficiently gentle; i.e., they must have large radii of curvature.³ If applications should require sharper bends, then the helical waveguide configuration will not be suitable. One solution, proposed by Irzinski, Krill, and Zinger,⁸ is to insert four commercially available rectangular waveguide bends between two of the transitions described above (Fig. 4). Currently, construction and testing of this waveguide "elbow" and the multiport rectangular-to-circular waveguide transitions are under way.

⁸E. P. Irzinski, J. A. Krill, and W. H. Zinger, "Sharp Mode-Transducer Bend for Overmoded Waveguide," U.S. Patent No. 4,679,008 (4 Aug 1987).

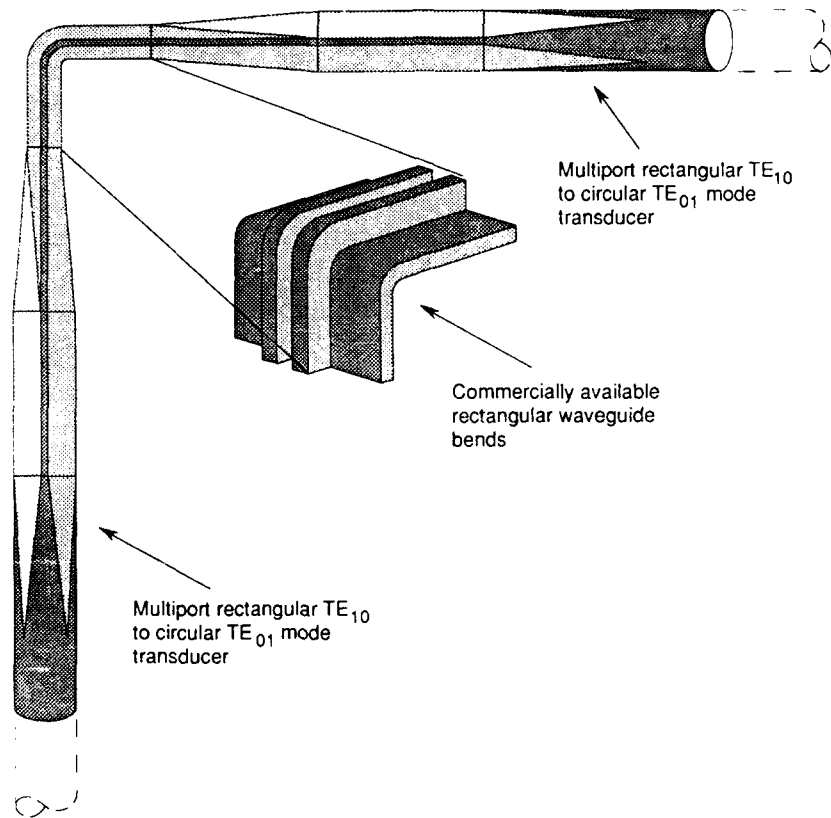


Figure 4 Mode-transducing elbow.

One rectangular-to-circular waveguide transition, the Marie transducer, has been built, analyzed, and tested.^{4,9} This device, which has been described as "the best transition to TE₀₁,"¹⁰ is shown in Fig. 5, and the electric field lines of the desired mode are shown in Fig. 6. Both the Marie transducer and the multiport transition consist, in part, of a transition between circular and cross-shaped waveguide. Because of this, the Marie transducer has been cited as the archetype for the transitions described above.⁷ One characteristic of the Marie transducer that may make it unsuitable for high-power use is that it has only one rectangular port.

A study of waveguide transition operation is under way. Design objectives for transitions built at APL include low levels of mode conversion and high power-carrying capability. In order to achieve these goals, it is necessary to thoroughly understand the theory of waveguide transition operation, to develop analytical techniques for the prediction of waveguide transition performance, and to validate such analytical techniques through extensive tests. Section 2 of this report discusses previous theoretical work on waveguide transitions. Section 3 briefly describes work done

⁴S. S. Saad, J. B. Davies, and O. J. Davies, "Computer Analysis of Gradually Tapered Waveguide with Arbitrary Cross Sections," *IEEE Trans. Microwave Theory and Techniques* **MTT-26**, 437-440 (May 1977).

¹⁰T. N. Anderson, "Low Loss Transmission Using Overmoded Waveguide: A Practical 1981 Review of the State of the Art," *IEEE AP/MTT-S Philadelphia Section Benjamin Franklin 1981 Symp. on Adv. in Antenna and Microwave Technol.*, Philadelphia (16 May 1981).

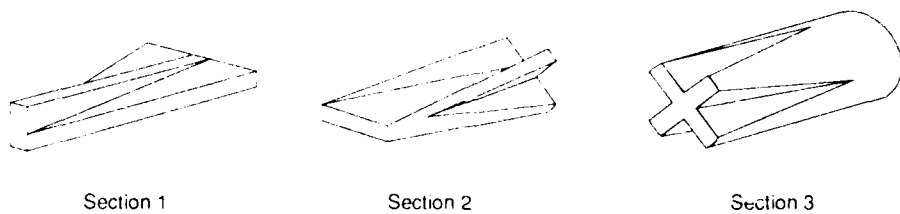


Figure 5 The Marie transducer

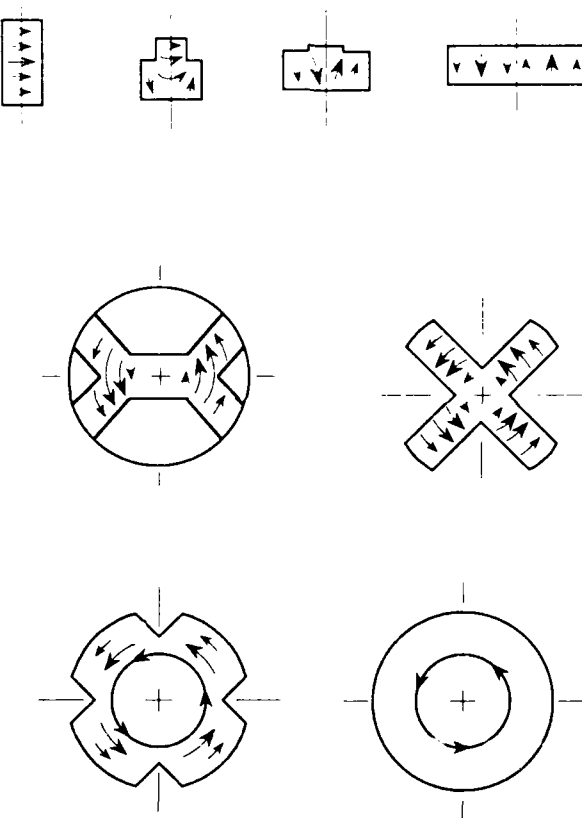


Figure 6 Desired electric fields lines for the Marie transducer.

at APL on computer programs based on this theoretical work. Future reports will discuss validation of these computer programs using scattering parameter tests and will describe a computer-aided design package for waveguide transitions. Specific transitions to be treated include the Marie transducer, the multiport rectangular TE_{10} to circular TE_{01} mode transducer, and the mode-transducing elbow. Section 4 of the report discusses future work and identifies several anticipated problem areas.

2. WAVEGUIDE TRANSITION THEORY

One of the earliest theoretical treatments of nonuniform waveguides was given by Reiter,⁵ who used the well-known fact that uniform waveguide modal fields form a complete orthogonal basis for physically realizable electromagnetic fields in a waveguide.¹¹ Extending this concept to waveguide transitions (Fig. 7), he asserted that the transverse electromagnetic field (i.e., the x and y components) could be written as a sum of the transverse fields of the uniform modes corresponding to the local waveguide transition cross section,⁵

$$\mathbf{E}_t(x,y,z) = \sum_{m=1}^{\infty} V_m(z) \mathbf{e}_m(x,y,z) \quad (1)$$

and

$$\mathbf{H}_t(x,y,z) = \sum_{m=1}^{\infty} I_m(z) \mathbf{h}_m(x,y,z) , \quad (2)$$

where \mathbf{E}_t is the transverse electric field,
 \mathbf{H}_t is the transverse magnetic field,
 \mathbf{e}_m is the transverse electric field of the m th uniform waveguide mode (suitably normalized),
 \mathbf{h}_m is the transverse magnetic field of the m th uniform waveguide mode (suitably normalized),
 $V_m(z)$ is the so-called "equivalent voltage," and
 $I_m(z)$ is the so-called "equivalent current."

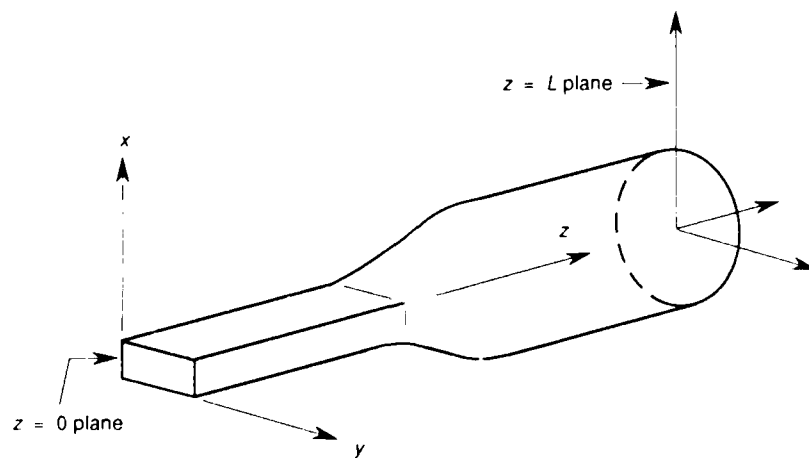


Figure 7 Generalized waveguide transition geometry

¹¹R. E. Collin, *Field Theory of Guided Waves*, McGraw-Hill Book Company, New York (1960).

The uniform waveguide modal transverse fields satisfy the orthonormality relations^{5,11}

$$\iint_S \mathbf{e}_i(x, y, z) \cdot \mathbf{e}_j(x, y, z) dx dy = \delta_{ij} \quad (3)$$

and

$$\iint_S \mathbf{h}_i(x, y, z) \cdot \mathbf{h}_j(x, y, z) dx dy = \delta_{ij} , \quad (4)$$

where the integration is over the local waveguide transition cross section and

$$\begin{aligned} \delta_{ij} &= 1 & i &= j , \\ \delta_{ij} &= 0 & \text{otherwise} . \end{aligned}$$

The equivalent voltages and currents are determined by an infinite set of ordinary differential equations:

$$\frac{dV_m}{dz} = -j\beta_m Z_m I_m + \sum_{n=1}^{\infty} T_{mn} V_n \quad (5)$$

and

$$\frac{dI_m}{dz} = -j\frac{\beta_m}{Z_m} V_m - \sum_{n=1}^{\infty} T_{nm} I_n , \quad (6)$$

respectively.

Both TE and TM modes are included in Eq. 5 and 6. The variable β_m denotes the wave number of the m th mode, the variable Z_m denotes the wave impedance of the m th mode, and the "transfer coefficients" T_{mn} (which describe coupling between the two modes m and n) are given by⁵

$$T_{mn}(z) = \iint_S \frac{d\mathbf{e}_m}{dz} \cdot \mathbf{e}_n dx dy . \quad (7)$$

The integration is over the local waveguide cross section. Equations 5 and 6 are known as the Generalized Telegraphist's Equations. Most methods of solving these equations start with a change of variables. Solymar proposed⁶

$$V_m = \sqrt{Z_m} (a_m^+ + a_m^-) \quad (8)$$

and

$$I_m = \frac{1}{\sqrt{Z_m}} (a_m^+ - a_m^-) , \quad (9)$$

where a_m^+ and a_m^- denote, respectively, the forward-traveling and the backward-traveling parts of the m th waveguide mode. Substitution of Eqs. 8 and 9 into Eqs. 5 and 6 results in a new system of ordinary differential equations. Solymar found an approximate solution to these equations for the case where no mode goes through cutoff inside the transition.⁶ Subsequently, Saad, Davies, and Davies used Solymar's solution to analyze the Marie transducer.^{4,9} Although several modes in the Marie transducer do, in fact, go through cutoff, thereby violating one of the key assumptions of Solymar's solution, rough agreement between theory and experiment was achieved.

The reason that some previous treatments avoid the case where a mode goes through cutoff inside the transition can be seen by examining Eqs. 8 and 9. In the plane where the mode goes through cutoff, the parameter $\sqrt{Z_m}$ in Eq. 8 will experience a singularity if the mode is TE, and the parameter $1/\sqrt{Z_m}$ in Eq. 9 will experience a singularity if the mode is TM. In order to circumvent this, our approach will be to solve Eqs. 5 and 6 directly. By truncating the series in Eqs. 5 and 6, the equations are cast into a form amenable to well-known numerical techniques (e.g., Ref. 12).

Two studies have, in fact, examined the solution of Eqs. 5 and 6 in some detail.^{13,14} Two Marie transducers are available for testing. Once such tests have been used to verify the numerical methods, it should be possible to develop a computer-aided design package for waveguide transitions. A prerequisite for such a study is the ability to specify the uniform waveguide modes associated with the various transition cross sections. Specifically, the modal electromagnetic fields are needed to compute the transfer coefficients of Eq. 7. A computer program that determines modal eigenvalues and electromagnetic fields is described in Section 3 of this report.

We conclude the present discussions by reviewing Reiter's derivation of Eqs. 5 and 6.⁵ (We present this derivation because Ref. 5 is not very widely available in the United States.)

The first step in deriving the Generalized Telegraphist's Equations (Eqs. 5 and 6) is to resolve the electromagnetic fields and the del operator into longitudinal and transverse components:

$$\begin{aligned}\mathbf{E} &= \mathbf{E}_t + \mathbf{z}E_z \\ \mathbf{H} &= \mathbf{H}_t + \mathbf{z}H_z \\ \nabla &= \nabla_t + \mathbf{z}\frac{\partial}{\partial z}\end{aligned}\tag{10}$$

¹²R. W. Hamming, *Numerical Methods for Scientists and Engineers*, McGraw-Hill Book Company, New York (1962).

¹³H. Flügel and E. Kühn, "Computer-Aided Analysis and Design of Circular Waveguide Tapers," *IEEE Trans. Microwave Theory and Techniques* **MTT-36**, 332-336 (1988).

¹⁴W. A. Huting and K. J. Webb, "Numerical Solution of the Continuous Waveguide Transition Problem," *IEEE Trans. Microwave Theory and Techniques* (to be published in November 1989).

The longitudinal components can be eliminated from Maxwell's Equations to obtain (e.g., Ref. 15, p. 186)

$$-\frac{\partial \mathbf{E}_t}{\partial z} = j\omega\mu(\mathbf{H}_t \times \mathbf{z}) - \frac{1}{j\omega\epsilon} \nabla_t \cdot [\nabla_t \cdot (\mathbf{H}_t \times \mathbf{z})] \quad (11)$$

and

$$-\frac{\partial \mathbf{H}_t}{\partial z} = j\omega\epsilon(\mathbf{z} \times \mathbf{E}_t) - \frac{1}{j\omega\mu} \nabla_t \cdot [\nabla_t \cdot (\mathbf{z} \times \mathbf{E}_t)] . \quad (12)$$

The basic procedure in this derivation is to insert the series expansions for \mathbf{E}_t and \mathbf{H}_t (Eqs. 1 and 2) into Eqs. 11 and 12 and to take advantage of the orthonormality relations given in Eqs. 3 and 4. The last two relationships allow us to determine the equivalent voltages and currents,

$$V_m(z) = \iint_S \mathbf{E}_t(x, y, z) \cdot \mathbf{e}_m(x, y, z) dx dy \quad (13)$$

and

$$I_m(z) = \iint_S \mathbf{H}_t(x, y, z) \cdot \mathbf{h}_m(x, y, z) dx dy , \quad (14)$$

respectively.

As before, the integrations are performed over the local waveguide transition cross section.

The basis functions \mathbf{e}_m and \mathbf{h}_m have several helpful properties. First of all, these vectors are related by a simple vector cross product,

$$\mathbf{h}_m(x, y, z) = \mathbf{z} \times \mathbf{e}_m(x, y, z) . \quad (15)$$

Also, by using Eqs. 41, 43, 44, and 46 (which are presented later), one obtains the following equations for TM and TE uniform waveguide modes,

$$\nabla_t \cdot [\nabla_t \cdot \mathbf{e}_{m,TM}(x, y, z)] + h_{m,TM}^2 \mathbf{e}_{m,TM}(x, y, z) = 0 \quad (16)$$

and

$$\nabla_t \cdot [\nabla_t \cdot \mathbf{h}_{m,TE}(x, y, z)] + h_{m,TE}^2 \mathbf{h}_{m,TE}(x, y, z) = 0 \quad (17)$$

¹⁵L. B. Felsen and N. Marcuvitz, *Radiation and Scattering of Waves*, Prentice-Hall, Inc., Englewood Cliffs, N.J. (1973).

We now derive Eq. 6 for the case where the subscript m denotes a TM uniform waveguide mode. Taking the dot product of Eq. 12 with $\mathbf{h}_{m,TM}$, and using Eq. 13, one finds that

$$\begin{aligned} & - \iint_S \frac{\partial \mathbf{H}_t}{\partial z} \cdot \mathbf{h}_{m,TM} \, dx \, dy \\ & = j\omega\epsilon V_{m,TM} - \frac{1}{j\omega\mu} \iint_S \nabla_t [\nabla_t \cdot (\mathbf{z} \times \mathbf{E}_t)] \cdot \mathbf{h}_{m,TM} \, dx \, dy. \end{aligned} \quad (18)$$

It will now be shown that the integral on the right-hand side of Eq. 18 vanishes. To do this, one applies the two-dimensional form of Green's theorem (e.g., Ref. 15, p. 188),

$$\begin{aligned} & \iint_S ds (\mathbf{A} \cdot \nabla_t \nabla_t \cdot \mathbf{B} - \mathbf{B} \cdot \nabla_t \nabla_t \cdot \mathbf{A}) \\ & = \oint_C dl [(\mathbf{A} \cdot \mathbf{n})(\nabla_t \cdot \mathbf{B}) - (\mathbf{B} \cdot \mathbf{n})(\nabla_t \cdot \mathbf{A})], \end{aligned} \quad (19)$$

where \mathbf{n} is the outward unit normal on the contour C . Substituting Eq. 19 into the integral on the right-hand side of Eq. 18 results in

$$\begin{aligned} & \iint_S \nabla_t [\nabla_t \cdot (\mathbf{z} \times \mathbf{E}_t)] \cdot \mathbf{h}_{m,TM} \, dx \, dy \\ & = \iint_S (\mathbf{z} \times \mathbf{E}_t) \cdot \nabla_t (\nabla_t \cdot \mathbf{h}_{m,TM}) \, dx \, dy \\ & + \oint_C (\mathbf{h}_{m,TM} \cdot \mathbf{n}) \nabla_t \cdot (\mathbf{z} \times \mathbf{E}_t) \, dl \\ & - \oint_C [(\mathbf{z} \times \mathbf{E}_t) \cdot \mathbf{n}] \nabla_t \cdot \mathbf{h}_{m,TM} \, dl. \end{aligned} \quad (20)$$

From the Maxwell divergence equation for \mathbf{B} , the first and third integrals vanish. The second integral also vanishes because $\mathbf{h}_{m,TM}$ satisfies the boundary condition for a perfect electrical conductor on C .

Inserting Eq. 2 into the left-hand side of Eq. 18, and taking note of Eq. 14, results in

$$\frac{dI_{m,TM}}{dz} = -j\omega\epsilon V_{m,TM} - \sum_{n=1}^{\infty} I_n \iint_S \frac{d\mathbf{h}_n}{dz} \cdot \mathbf{h}_{m,TM} \, dx \, dy. \quad (21)$$

Remembering Eqs. 7 and 15, one can show that Eqs. 6 and 21 are equivalent by substituting the following expressions:

$$\beta_m = \sqrt{\omega^2 \mu \epsilon - h_m^2} \quad (22)$$

and

$$Z_{m,TM} = \frac{\beta_{m,TM}}{\omega\epsilon} \quad (23)$$

Equation 22 applies to both TE and TM modes. Therefore, the subscript TM has been dropped. The eigenvalue h_m (not to be confused with the modal magnetic field \mathbf{h}_m) is given in Eqs. 16 and 17 and in Eqs. 41 and 44 (which appear later). We now seek to derive Eq. 5 for the case where m denotes a TM mode. Proceeding as before, Eqs. 11 and 14 are combined to yield:

$$\begin{aligned} & - \iint_S \frac{\partial \mathbf{E}_t}{\partial z} \cdot \mathbf{e}_{m,TM} \, dx \, dy \\ &= j\omega\mu I_{m,TM} - \frac{1}{j\omega\epsilon} \iint_S \nabla_t [\nabla_t \cdot (\mathbf{H}_t \times \mathbf{z})] \cdot \mathbf{e}_{m,TM} \, dx \, dy. \end{aligned} \quad (24)$$

Unfortunately, the integral on the right-hand side of Eq. 24 does not vanish. Using Green's theorem (Eq. 19),

$$\begin{aligned} & \iint_S \mathbf{e}_{m,TM} \cdot \nabla_t [\nabla_t \cdot (\mathbf{H}_t \times \mathbf{z})] \, dx \, dy \\ &= \iint_S (\mathbf{H}_t \times \mathbf{z}) \cdot \nabla_t (\nabla_t \cdot \mathbf{e}_{m,TM}) \, dx \, dy \\ &+ \oint_C (\mathbf{e}_{m,TM} \cdot \mathbf{n}) \nabla_t \cdot (\mathbf{H}_t \times \mathbf{z}) \, dl \\ &- \oint_C [(\mathbf{H}_t \times \mathbf{z}) \cdot \mathbf{n}] \nabla_t \cdot \mathbf{e}_{m,TM} \, dl. \end{aligned} \quad (25)$$

Using the simple vector identity $\mathbf{A} \cdot (\mathbf{B} \times \mathbf{C}) = \mathbf{B} \cdot (\mathbf{C} \times \mathbf{A})$, and using Eqs. 14, 15, and 16, the first term on the right-hand side of Eq. 25 is seen to be

$$\iint_S \mathbf{H}_t \times \mathbf{z} \cdot \nabla_t (\nabla_t \cdot \mathbf{e}_{m,TM}) \, dx \, dy = -h_{m,TM}^2 I_{m,TM}. \quad (26)$$

Applying the Maxwell curl equation for \mathbf{H} to the second term on the right-hand side of Eq. 25, one obtains

$$\oint_C (\mathbf{e}_{m,TM} \cdot \mathbf{n}) \nabla_t \cdot (\mathbf{H}_t \times \mathbf{z}) \, dl = \oint_C (\mathbf{e}_{m,TM} \cdot \mathbf{n}) j\omega\epsilon E_z \, dl. \quad (27)$$

From Fig. 8, one obtains the electric field boundary condition,

$$E_z = -(\tan \phi) \mathbf{E}_t \cdot \mathbf{n}. \quad (28)$$

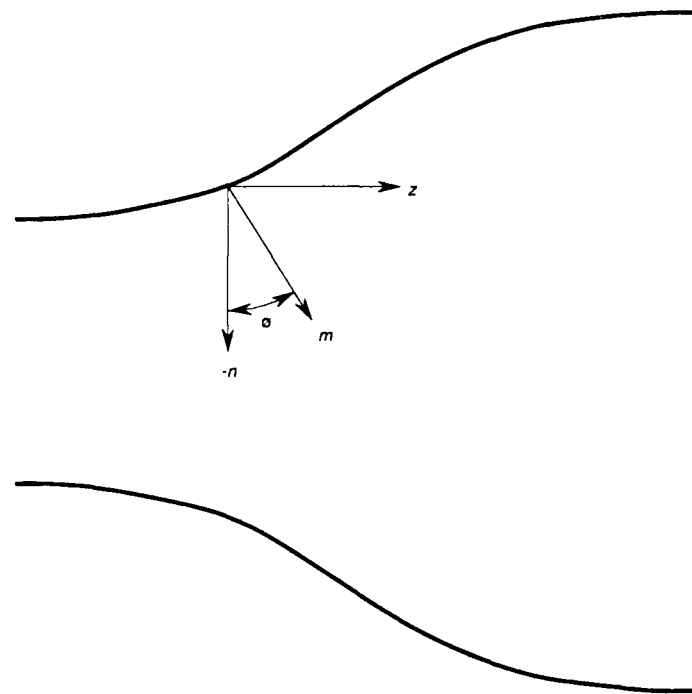


Figure 8 Waveguide transition geometry for electromagnetic field boundary conditions.

Equation 28 follows from the requirement that the electric field tangent to a perfect conductor must vanish. Inserting Eq. 28 into Eq. 27, and noting that $\mathbf{e}_{m,TM}$ is parallel to \mathbf{n} , one finds that

$$\oint_C (\mathbf{e}_{m,TM} \cdot \mathbf{n}) \nabla_t \cdot (\mathbf{H}_t \times \mathbf{z}) \, dl = -j\omega\epsilon \oint_C (\tan \phi) \mathbf{E}_t \cdot \mathbf{e}_{m,TM} \, dl. \quad (29)$$

Finally, the third term on the right-hand side of Eq. 25 is seen to vanish if one applies the Maxwell divergence equation to $\mathbf{e}_{m,TM}$ and uses the electromagnetic boundary conditions for a perfect electrical conductor. Combining Eqs. 24, 25, 26, and 29 yields

$$\begin{aligned} & - \iint_S \frac{\partial \mathbf{E}_t}{\partial z} \cdot \mathbf{e}_{m,TM} \, dx \, dy \\ & = (j\omega\mu + \frac{h_{m,TM}^2}{j\omega\epsilon}) I_{m,TM} + \oint_C (\tan \phi) \mathbf{E}_t \cdot \mathbf{e}_{m,TM} \, dl. \end{aligned} \quad (30)$$

We treat the term on the left-hand side of Eq. 30 by invoking the differentiation theorem of surface integrals with variable surface,

$$\frac{d}{dz} \iint_S x(x, y, z) \, dx \, dy = \iint_S \frac{\partial x}{\partial z} \, dx \, dy + \oint_C x (\tan \phi) \, dl. \quad (31)$$

Using this theorem, the left-hand side of Eq. 30 becomes

$$-\iint_S \frac{\partial \mathbf{E}_t}{\partial z} \cdot \mathbf{e}_{m,TM} \, dx \, dy = -\frac{d}{dz} \iint_S \mathbf{E}_t \cdot \mathbf{e}_{m,TM} \, dx \, dy \\ + \iint_S \mathbf{E}_t \cdot \frac{\partial \mathbf{e}_{m,TM}}{\partial z} \, dx \, dy + \oint_C (\tan \phi) \mathbf{E}_t \cdot \mathbf{e}_{m,TM} \, dl. \quad (32)$$

Combining Eqs. 13, 30, and 32 results in

$$-\frac{dV_{m,TM}}{dz} = \left(j\omega\mu + \frac{h_{m,TM}^2}{j\omega\epsilon} \right) I_{m,TM} - \sum_{n=1}^{\infty} V_n \iint_S \mathbf{e}_n \cdot \frac{\partial \mathbf{e}_{m,TM}}{\partial z} \, dx \, dy. \quad (33)$$

Equations 7, 22, and 23 can be used to show that this result is equivalent to Eq. 5.

Reiter's derivation of Eqs. 5 and 6 for the case where m denotes a TE mode is quite similar to the foregoing, and will not be given here. The expression for a TE mode wave impedance is

$$Z_{m,TE} = \frac{\omega\mu}{\beta_{m,TE}}. \quad (34)$$

Before concluding this section, let us consider the convergence of the series representations of the electric and magnetic fields and how such convergence is affected by the electromagnetic field boundary conditions. At the boundary of the transition, the fields satisfy the conditions (Fig. 8)

$$\mathbf{E} \times \mathbf{m} = 0 \quad (35)$$

and

$$\mathbf{H} \cdot \mathbf{m} = 0. \quad (36)$$

Decomposing these requirements into longitudinal and transverse parts, we find that

$$\mathbf{n} \times \mathbf{E}_t = 0, \quad (37)$$

$$E_z = -(\tan \phi) \mathbf{E}_t \cdot \mathbf{n}, \quad (27)$$

and

$$H_z = (\cot \phi) \mathbf{H}_t \cdot \mathbf{n}. \quad (38)$$

The boundary conditions satisfied by the vector functions \mathbf{e}_m and \mathbf{h}_m (the modal fields of a uniform waveguide) are

$$\mathbf{n} \times \mathbf{e}_m = 0 \quad (39)$$

and

$$\mathbf{n} \cdot \mathbf{h}_m = 0 . \quad (40)$$

Thus boundary condition Eq. 37 for the transverse electric field is satisfied by the individual terms of the series in Eq. 1. Therefore, following the approach of Ref. 16, we assume that the expansion is valid both in the interior of S and on C (the boundary of S). This is not the case for the magnetic field. The individual terms of this series satisfy Eq. 40 but the actual magnetic field must satisfy Eq. 38. Again following the approach of Ref. 16, the series in Eq. 2 is assumed to be a valid representation for \mathbf{H}_t in the interior of S but not on the boundary of S . In the union of S and its boundary, the series of Eq. 2 will represent a discontinuous function and hence will not converge uniformly. Because of this, term-by-term differentiation with respect to x or y will certainly make the series diverge. However, such differentiation has been avoided in the above derivation. Term-by-term integration has not been avoided, but the conditions for the validity of this procedure are not stringent (e.g., Ref. 17, pp. 40-43 and 345-347). These general conclusions—namely, that one field series is valid on the boundary but that the other field series is not—have been noted in other treatments of nonuniform waveguide theory.^{16,18}

¹⁶A. F. Stevenson, "General Theory of Electromagnetic Horns," *J. Appl. Phys.* **22**, 1447-1460 (1951).

¹⁷E. C. Titchmarsh, *The Theory of Functions*, 2nd ed., Oxford University Press, London (1939).

¹⁸H.-G. Unger, "Circular Waveguide Taper of Improved Design," *Bell Syst. Tech. J.* **37**, 899-912 (1958).

3. COMPUTER SOFTWARE DEVELOPMENT

The ability to calculate the modal fields and wave numbers associated with uniform waveguides is a prerequisite for solving the system of differential equations described in Section 2. This has to be done for a wide variety of waveguide cross sections. This section lists the equations that determine the modal fields, describes numerical techniques for solving these equations, and describes work done at APL in this area. For a TM mode, the starting point in specification of the fields is to solve the two-dimensional Helmholtz equation with Dirichlet boundary conditions,

$$\nabla_t^2 \psi_{m,TM} + h_{m,TM}^2 \psi_{m,TM} = 0 \quad (41)$$

and

$$\psi_{m,TM} = 0 \quad \text{on } C. \quad (42)$$

The transverse field functions and the wave number may be found from

$$\mathbf{e}_{m,TM} = \nabla_t \psi_{m,TM}, \quad (43)$$

$$\mathbf{h}_m = \mathbf{z} \times \mathbf{e}_m, \quad (15)$$

and

$$\beta_m = \sqrt{\omega^2 \mu \epsilon - h_m^2}. \quad (22)$$

The equations for the modal magnetic field \mathbf{h}_m and the wave number β_m apply to both TE and TM modes. Therefore, the subscript TM has been dropped. For TE fields, one starts with the Helmholtz equations with Neumann boundary conditions,

$$\nabla_t^2 \psi_{m,TE} + h_{m,TE}^2 \psi_{m,TE} = 0 \quad (44)$$

and

$$\frac{\partial \psi_{m,TE}}{\partial n} = 0 \quad \text{on } C. \quad (45)$$

The wave number may be found from Eq. 22 and the field functions may be obtained through

$$\mathbf{h}_{m,TE} = \nabla_t \psi_{m,TE} \quad (46)$$

and

$$\mathbf{e}_m = \mathbf{h}_m \times \mathbf{z} . \quad (47)$$

One procedure that can be used to solve the Helmholtz equation numerically is the finite element method (FEM). An FEM package has been ordered from McGill University and installed at APL on an Amdahl 5890 computer system. Validation of this package has been accomplished by solving waveguide problems with known closed-form solutions. For descriptions of the FEM method, see Refs. 19-22. In order to run the McGill University FEM package, it is necessary to approximate the waveguide cross section as a union of triangles (Fig. 9). This package does not have

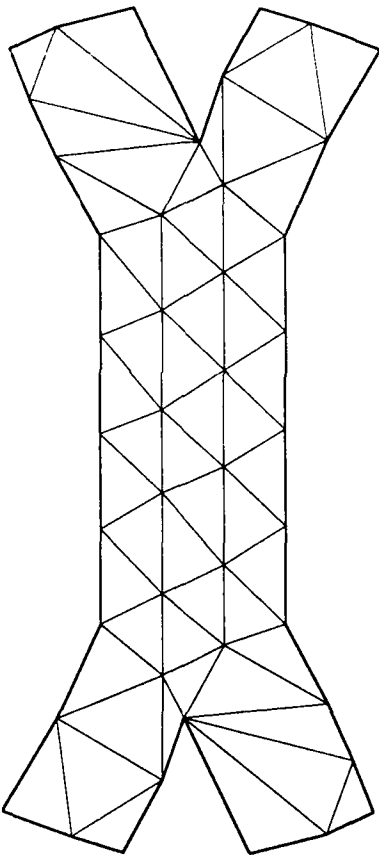


Figure 9 Waveguide cross section approximated as a union of triangles.

¹⁹A. Konrad and P. P. Sylvester, "Scalar Finite-Element Package for Two-Dimensional Field Problems," *IEEE Trans. Microwave Theory and Techniques MTT-19*, 952-954 (1971).

²⁰P. P. Sylvester, "A General High-Order Finite-Element Waveguide Analysis Program," *IEEE Trans. Microwave Theory and Techniques MTT-17*, 204-210 (1969).

²¹P. P. Sylvester, "High-Order Polynomial Triangular Finite Elements for Potential Problems," *International J. Eng. Sci.* 7, 849-861 (1969).

²²P. P. Sylvester and R. L. Ferrari, *Finite Elements for Electrical Engineers*, Cambridge University Press, New York (1983).

a routine for generating these triangles but instead depends on user-generated input. For the large number of waveguide cross sections to be treated in our work, the triangle-generating process is complicated and formidable. Software that generates such triangles has been ordered from Los Alamos National Laboratory and installed on the Amdahl system. This triangle-generator (or "mesh generator") is part of a finite-difference package called POISSON/SUPERFISH, which was developed for the Department of Energy for the purpose of solving magnetostatic and electrostatic problems and RF cavity problems.^{23,24} The two routines that are relevant to our work are AUTOMESH and LATTICE. AUTOMESH reads in boundary data and mesh size specifications and prepares a preliminary mesh. LATTICE uses the method of Ref. 25 to refine the mesh. AUTOMESH has been successfully tested by running example problems from Ref. 23. Testing of the routine LATTICE is under way.

Once work is complete on the mesh generator and the FEM package, we will be able to analyze waveguide transitions by performing a uniform waveguide analysis for some large number M of waveguide transition cross sections (Fig. 10). The vector functions e_m can be found by taking the gradient of the solutions to the Helmholtz equation. Since the FEM package approximates these solutions as polynomials in x and y , analytical instead of numerical differentiation will be used. Numerical differentiation will have to be used in differentiating e_m with respect to z (Eq. 7). Finally, the integration of Eq. 7 and the ultimate solution of the truncated system of differential equations will also have to be accomplished numerically.

Figure 11 shows a flow chart for computing the transmission and reflection properties of a waveguide transition. To summarize, the first step in analyzing a waveguide transition is to solve the uniform waveguide problem for some large number M of transition cross sections. The routines AUTOMESH and LATTICE approximate each cross section as a union of triangles. The FEM package then solves for the uniform waveguide modes. Finally, the transfer coefficients (Eq. 7) are integrated numerically, and the system of differential equations is truncated and solved. To date, the mesh generation package and the FEM package have been installed at APL and tested. Future work includes implementation of routines to set up and solve the system of differential equations.^{13,14}

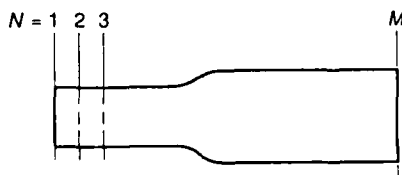


Figure 10 Nonuniform waveguide with transverse planes.

²³M. T. Menzel and H. K. Stokes, "User's Guide for the POISSON/SUPERFISH Group of Codes," Los Alamos National Laboratory LA-UR-87-115 (Jan 1987).

²⁴J. L. Warren, G. Boicourt, M. Foss, B. Tice, M. T. Menzel, and H. K. Stokes, "Reference Manual for the POISSON/SUPERFISH Group of Codes," Los Alamos National Laboratory LA-UR-87-126 (Jan 1987).

²⁵A. M. Winslow, "Numerical Solution of the Quasilinear Poisson Equation for a Nonuniform Mesh," *J. Computational Phys.* 1, 149-172 (1966).

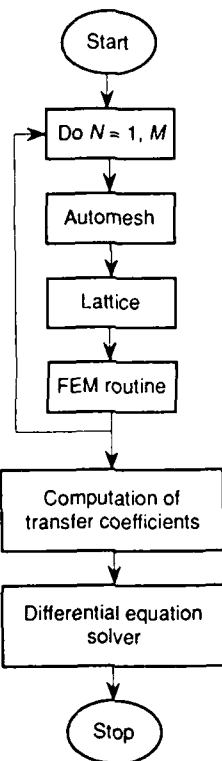


Figure 11 Computer program package for scattering matrix determination.

4. FUTURE WORK

As previously mentioned, future work includes completion of the computer software development, experimental validation of the computer programs by scattering parameter measurements, and development of a computer-aided design procedure. Specific transitions to be treated include the Marie transducer, the multiport transition, and the mode-transducing elbow. To date, the following tasks and problem areas have been identified:

1. Uniform Waveguide Mode Computation

Development of the routine LATTICE must be finished. Once this is done, the uniform waveguide modes for two Marie transducers will be computed, along with the associated transfer coefficients.

2. Solution of the System of Ordinary Differential Equations

In order to specify the transmission and reflection properties of a waveguide transition, Eqs. 5 and 6 must be solved. The methods described in Refs. 13 and 14 will be studied for possible applicability to the complicated transitions described in Section 1.

3. Mode conversion at a Metallic/Helical Waveguide Interface

The ultimate goal for this project is to efficiently couple energy into a round overmoded sheathed-helix waveguide. The junction between a metallic waveguide transition and a helical waveguide presents a sharp discontinuity to the electromagnetic waves, causing mode conversion and reflections.²⁶

4. Computation of the Transmission and Reflection Properties of a Waveguide Transition

The scattering matrix of a metallic waveguide transition is specified by solving Eqs. 5 and 6. Two Marie transducers are available to us for testing using an HP 8409C automatic network analyzer. In all tests, the Marie transducers will be connected to each other either by a plain copper circular waveguide or by a sheathed-helix waveguide. We hope to achieve better agreement between theory and experiment than was possible in the past.^{4,9}

5. Multiport Transition Analysis and Design

Analyze the multiport rectangular TE_{10} to circular TE_{01} mode transducer and the mode transducing elbow. As before, the analysis will be accomplished by solving Eqs. 5 and 6. The four rectangular bends in the elbow will be analyzed by solving the differential equations given by Schelkunoff.²⁷

6. Spurious Mode Resonances

In a multimode waveguide system, the presence of a region that can support one or more spurious modes can lead to high transmission loss at frequencies for which the region is resonant for one of these modes.²⁸ Previous designs of the Marie transducer have sought to eliminate such resonances by eliminating some of the spurious mode-supporting regions (Figs. 12 and 13).^{4,29,30} One such region that cannot be eliminated, of course, is the circular overmoded waveguide itself. Reference 28 in-

²⁶J. W. Lechleider, "Mode Conversion at the Junction of Helix Waveguide and Copper Pipe," *Bell Syst. Tech. J.* **38**, 1317-1329 (1959).

²⁷S. A. Schelkunoff, "Conversion of Maxwell's Equations into Generalized Telegraphist's Equations," *Bell Syst. Tech. J.* **34**, 995-1043 (1955).

²⁸A. P. King and E. A. Marcatili, "Transmission Loss due to Resonance of Loosely Coupled Modes in a Multimode System," *Bell Syst. Tech. J.* **35**, 899-906 (1956).

²⁹Y. M. Isayenko, " H_{10} - H_{01} - H_{01} Continuous Transformer," *Proc. Third Colloquium on Microwave Communication*, Budapest, Hungary, pp. 467-475 (Apr. 1966).

³⁰S. S. Saad, J. B. Davies, and O. J. Davies, "Analysis and Design of a Circular TE_{01} Mode Transducer," *IEE J. Microwaves, Opt. and Acoust.* **1**, 58-62 (1977).

dicates that mode-suppressing circular waveguide tends to lower the quality factor, Q , of these resonances, thereby flattening frequency responses. In order to completely eliminate this type of loss, spurious mode resonances must be located sufficiently far outside the operating band so that this flattening effect does not degrade performance.

7. High Power Considerations

High power transmission can lead to two undesirable effects in waveguide transitions: excessive heat losses inside the wall of the transition, and electrical breakdown within the air inside the transition. Design rules for maximizing power-carrying capability are sought as part of this study.

8. Design procedure for Waveguide Transitions

One objective of this study is to develop a computer-aided design package for rectangular-to-circular waveguide transitions such as the Marie transducer and the multiport transition. This package should be capable of dealing with tradeoffs among the goals of maximum power-carrying capability, low reflectivity, low transmission loss, low mode conversion, minimum transition physical length, and location of the spurious mode resonances outside the operating band.

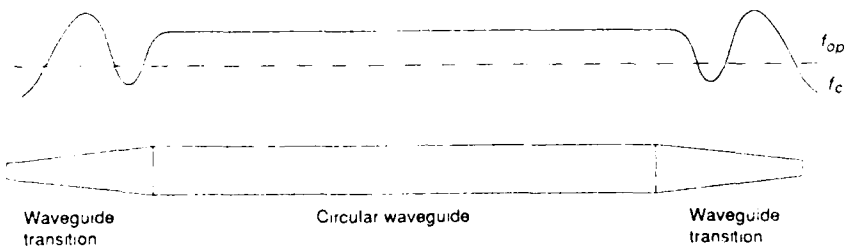


Figure 12 Waveguide run with regions capable of supporting a spurious mode. The spurious mode cutoff frequency is shown as a function of position.

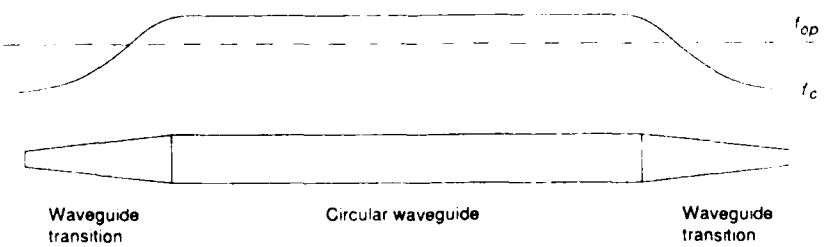


Figure 13 Waveguide run in which some of the spurious mode resonances have been eliminated. Note that two of the possible resonant regions are no longer present.

ACKNOWLEDGMENT

The author is grateful to Dr. Kevin J. Webb of the University of Maryland for many helpful discussions and suggestions.

REFERENCES

- 1 W. A. Huting, J. A. Krill, and K. J. Webb, "New Developments in Circular Overmoded Waveguide," in *1988 URSI Radio Science Meeting Programs and Abstracts*, International Union of Radio Science, Syracuse, N.Y., p. 202 (1988).
- 2 H. E. Rowe and W. D. Warters, "Transmission in Multimode Waveguide with Random Imperfections," *Bell Syst. Tech. J.* **41**, 1031-1170 (1962).
- 3 H.-G. Unger, "Normal Mode Bends for Circular Electric Waves," *Bell Syst. Tech. J.* **36**, 1292-1307 (1957).
- 4 S. S. Saad, "Computer Analysis and Design of Gradually Tapered Waveguide with Arbitrary Cross Sections," Ph.D. dissertation, University College, London (Oct 1973).
- 5 G. Reiter, "Generalized Telegraphist's Equation for Waveguides of Varying Cross Sections," *Proc. IEE* **106B**, Suppl. 13, 54-57 (1959).
- 6 L. Solymar, "Spurious Mode Generation in Nonuniform Waveguide," *IRE Trans. Microwave Theory and Techniques* **MTT-7**, 379-383 (1959).
- 7 W. H. Zinger and J. A. Krill, "Multiport Rectangular TE_{10} to Circular TE_{01} Mode Transducer Having Pyramidal Shaped Transducing Means," U.S. Patent No. 4,628,287 (9 Dec 1986).
- 8 E. P. Irzinski, J. A. Krill, and W. H. Zinger, "Sharp Mode-Transducer Bend for Overmoded Waveguide," U.S. Patent No. 4,679,008 (14 Aug 1987).
- 9 S. S. Saad, J. B. Davies, and O. J. Davies, "Computer Analysis of Gradually Tapered Waveguide with Arbitrary Cross Sections," *IEEE Trans. Microwave Theory and Techniques* **MTT-26**, 437-440 (May 1977).
- 10 T. N. Anderson, "Low Loss Transmission Using Overmoded Waveguide: A Practical 1981 Review of the State of the Art," IEEE AP/MTT-S Philadelphia Section Benjamin Franklin 1981 Symp. on Adv. in Antenna and Microwave Technol., Philadelphia (16 May 1981).
- 11 R. E. Collin, *Field Theory of Guided Waves*, McGraw-Hill Book Company, New York (1960).
- 12 R. W. Hamming, *Numerical Methods for Scientists and Engineers*, McGraw-Hill Book Company, New York (1962).
- 13 H. Flügel and E. Kühn, "Computer-Aided Analysis and Design of Circular Waveguide Tapers," *IEEE Trans. Microwave Theory and Techniques* **MTT-36**, 332-336 (1988).
- 14 W. A. Huting and K. J. Webb, "Numerical Solution of the Continuous Waveguide Transition Problem," submitted to *IEEE Trans. Microwave Theory and Techniques* (to be published in November 1989).
- 15 L. B. Felsen and N. Marcuvitz, *Radiation and Scattering of Waves*, Prentice-Hall, Inc., Englewood Cliffs, N.J. (1973).

- ¹⁶A. F. Stevenson, "General Theory of Electromagnetic Horns," *J. Appl. Phys.* **22**, 1447-1460 (1951).
- ¹⁷E. C. Titchmarsh, *The Theory of Functions*, 2nd ed., Oxford University Press, London (1939).
- ¹⁸H.-G. Unger, "Circular Waveguide Taper of Improved Design," *Bell Syst. Tech. J.* **37**, 899-912 (1958).
- ¹⁹A. Konrad and P. P. Sylvester, "Scalar Finite-Element Package for Two-Dimensional Field Problems," *IEEE Trans. Microwave Theory and Techniques MTT-19*, 952-954 (1971).
- ²⁰P. P. Sylvester, "A General High-Order Finite-Element Waveguide Analysis Program," *IEEE Trans. Microwave Theory and Techniques MTT-17*, 204-210 (1969).
- ²¹P. P. Sylvester, "High-Order Polynomial Triangular Finite Elements for Potential Problems," *International J. Eng. Sci.* **7**, 849-861 (1969).
- ²²P. P. Sylvester and R. L. Ferrari, *Finite Elements for Electrical Engineers*, Cambridge University Press, New York (1983).
- ²³M. T. Menzel and H. K. Stokes, "User's Guide for the POISSON/SUPERFISH Group of Codes," Los Alamos National Laboratory LA-UR-87-115 (Jan 1987).
- ²⁴J. L. Warren, G. Boicourt, M. Foss, B. Tice, M. T. Menzel, and H. K. Stokes, "Reference Manual for the POISSON/SUPERFISH Group of Codes," Los Alamos National Laboratory LA-UR-87-126 (Jan 1987).
- ²⁵A. M. Winslow, "Numerical Solution of the Quasilinear Poisson Equation for a Nonuniform Mesh," *J. Computational Phys.* **1**, 149-172 (1966).
- ²⁶J. W. Lechleider, "Mode Conversion at the Junction of Helix Waveguide and Copper Pipe," *Bell Syst. Tech. J.* **38**, 1317-1329 (1959).
- ²⁷S. A. Schelkunoff, "Conversion of Maxwell's Equations into Generalized Telegraphist's Equations," *Bell Syst. Tech. J.* **34**, 995-1043 (1955).
- ²⁸A. P. King and E. A. Marcatili, "Transmission Loss due to Resonance of Loosely Coupled Modes in a Multimode System," *Bell Syst. Tech. J.* **35**, 899-906 (1956).
- ²⁹Y. M. Isayenko, " H_{10} - H_{02} - H_{01} Continuous Transformer," *Proc. Third Colloquium on Microwave Communication*, Budapest, Hungary, pp. 467-475 (Apr 1966).
- ³⁰S. S. Saad, J. B. Davies, and O. J. Davies, "Analysis and Design of a Circular TE_{01} Mode Transducer," *IEE J. Microwaves, Opt. and Acoust.* **1**, 58-62 (1977).

INITIAL DISTRIBUTION EXTERNAL TO THE APPLIED PHYSICS LABORATORY*

* work reported in LG 1375 was done under Navy Contract N00039-89-C-5301 and is related to Task BKAR, supported by the NAVSEA.

ORGANIZATION	LOCATION	ATTENTION	No. of Copies
DEPARTMENT OF DEFENSE			
Secretary of Defense	Washington, DC 20301	G. C. Kopesak, OUSDRE (ET)	1
Office of the Under Secretary of Defense, Research and Engineering	Washington, DC 20301	J. MacCullum	1
Defense Technical Information Center	Alexandria, VA 23314	Accessions	12
Defense Advanced Research Projects Agency	Arlington, VA 20331	S. Karp	1
DEPARTMENT OF THE NAVY			
Chief of Naval Operations	Washington, DC 20350	OP 98 OP 983 OP 987 OP 987B OP 35 OP 35F OP 352L OP 355W OP 507D	1 1 1 2 1 1 1 1 1
Office of the Assistant Secretary of the Navy	Washington, DC 20350	E. Donaldson C. Kincaid R. E. Merry R. L. Rumpf W. C. Condell, Jr., ONR-421 E. Wegman, ONR-411SP CNT 07C ONT 0712 ONT 0713	1 1 1 1 1 1 1 1 1
Office of Naval Research	Arlington, VA 22217	AIR 320 AIR 320B AIR 320D AIR 320R AIR 340J AIR 06 AIR 0623 Library, AIR 7226	1 1 1 1 1 1 1 2
Office of Naval Technology	Arlington, VA 22209	B. Dillon G. Savoca S. Campana, 3011 D. M. Ferreira T. Tao T. G. Giallorenzi, 6500 J. Kershenstein, 6520 E. J. Stone, 6520	1 1 1 1 1 1 1 1
Naval Air Systems Command	Washington, DC 22202	Library SEA 06 SEA 06A SEA 06A1 SEA 06AX SEA 06P SEA 06R SEA 62 SEA62B	1 1 1 1 1 1 1 1 1
Naval Air Development Center Naval Electronic Systems Command Naval Postgraduate School Naval Research Laboratory	Warminster, PA 18974 Arlington, VA 20360 Monterey, CA 92940 Washington, DC 20375		
Space & Naval Warfare Systems Command Naval Sea Systems Command	Washington, DC 20360 Washington, DC 22202		

Requests for copies of this report from DoD activities and contractors should be directed to DTIC.
Cameron Station, Alexandria, Virginia 22314 using DTIC Form 1 and, if necessary, DTIC Form 55.

INITIAL DISTRIBUTION EXTERNAL TO THE APPLIED PHYSICS LABORATORY*

INITIAL DISTRIBUTION EXTERNAL TO THE APPLIED PHYSICS LABORATORY*

ORGANIZATION	LOCATION	ATTENTION	No. of Copies
CONTRACTORS			
Antennas for Communications	Ocala, FL 32678	W. H. Riesz	1
Charles Stark Draper Laboratory	Cambridge, MA 02139	T. H. Brooks	1
General Electric	Syracuse, NY 13221	A. F. Milton	1
General Research Corp.	McLean, VA 22101	R. Zirkind	1
Honeywell, Inc.	Minneapolis, MN 55440	P. M. Narendra	1
IBM Federal Systems Division	Westlake Village, CA 91361	J. C. Day	1
Institute for Defense Analyses	Alexandria, VA 22311	I. W. Kaye	1
Lockheed Missile and Space Co.	Palo Alto, CA 94304	L. H. Wald	1
MIT Lincoln Laboratory	Lexington, MA 02173	H. Kleiman	1
Rand Corporation	Santa Monica, CA 90406	L. G. Mundie	1
Raytheon Missile Systems Division	Bedford, MA 01730	J. Goldstein	1
Riverside Research Institute	New York, NY 10036	R. G. Cestaro	1
Rockwell International	Downey, CA 90241	M. F. Sentovich	1
Science Applications	Ann Arbor, MI 48104	R. Turner	1
Technology Service Corporation	Silver Spring, MD 20910	J. Hoffman	1
Purdue University	Lafayette, IN	G. W. Slade	1
Polytechnic University	Farmingdale, NY	K. J. Webb	1
		L. Carin	1